

- (40) (a) L. I. B. Haines, D. J. Hopgood, and A. J. Poë, *J. Chem. Soc. A*, 421 (1968);
 (b) J. P. Fawcett and A. Poë, *J. Chem. Soc., Dalton Trans.*, 1302 (1977).
 (41) M. S. Wrighton and D. S. Ginley, *J. Am. Chem. Soc.*, **97**, 2065 (1975).
 (42) R. A. Jackson and A. J. Poë, *Inorg. Chem.*, **17**, 997 (1978).
 (43) C. A. Tolman, *Chem. Rev.*, **77**, 313 (1977).
 (44) D. M. Allen, A. Cos, T. J. Kemp, Q. Sultanu, and R. B. Pitts, *J. Chem. Soc., Dalton Trans.*, 1189 (1976).
 (45) A. Hudson, M. F. Lappert, and B. K. Nicholson, *J. Organomet. Chem.*, **92**, C11 (1975).
 (46) M. Absi-Halabi and T. L. Brown, *J. Am. Chem. Soc.*, **99**, 2982 (1977).

Metal Clusters in Catalysis. 15.^{1a} A Structural and Chemical Study of a Dinuclear Metal Complex, $[\eta^3\text{-C}_3\text{H}_5\text{Fe}(\text{CO})_3]_2$

Charles F. Putnik,^{1b} James J. Welter,^{1b} Galen D. Stucky,^{*1b} M. J. D'Aniello, Jr.,^{1c} B. A. Sosinsky,^{1c} J. F. Kirner,^{1c} and E. L. Muetterties^{*1c}

Contribution from the Department of Chemistry and Materials Research Laboratory, University of Illinois at Urbana-Champaign, Urbana, Illinois 61801, and the Department of Chemistry and Cornell Materials Science Center, Cornell University, Ithaca, New York 14853. Received August 29, 1977

Abstract: The crystal and molecular structure of $[\eta^3\text{-C}_3\text{H}_5\text{Fe}(\text{CO})_3]_2$ crystallized from pentane at -78°C was solved from x-ray diffraction data collected from a single crystal. The crystals belong to the monoclinic space group $P2_1/n$ with unit cell dimensions $a = 8.356(7) \text{ \AA}$, $b = 9.400(9) \text{ \AA}$, $c = 9.315(9) \text{ \AA}$, $\beta = 91.13(2)^\circ$, $V = 731.42 \text{ \AA}^3$; $\rho_{\text{calcd}} = 1.643 \text{ g/cm}^3$ for $Z = 2$. Full-matrix least-squares refinement, including the third cumulant of probability density function of the structure factor equation, yielded an R factor of 0.069 and a weighted R factor of 0.049 for 1675 observed reflections. This dimeric iron complex lies on a crystallographic center of inversion and has a trans arrangement of the trihapto allyl ligands. The iron-iron distance is surprisingly long, $3.138(3) \text{ \AA}$, although this distance is consistent with the low enthalpy value for dimer dissociation in the solution phase. The coordination sphere about an iron atom may be best described as pseudooctahedral with the allyl ligand considered a bidentate ligand. In solution, $[\eta^3\text{-C}_3\text{H}_5\text{Fe}(\text{CO})_3]_2$ slowly decomposed to give an array of compounds: propene, $\text{Fe}(\text{CO})_5$, $\text{Fe}_3(\text{CO})_{12}$, and a set of three ferracyclopentadiene molecules. The metallacycles included tricarbonyl[tricarbonyl(2-ethylferracyclopentadiene)]iron (1), hexacarbonyl[dicarbonyl(2-ethylferracyclopentadiene)]diiron (2), and tricarbonyl[tricarbonyl(2-hydroxyferracyclopentadiene)]iron (3). Hydrogenation of $[\eta^3\text{-C}_3\text{H}_5\text{Fe}(\text{CO})_3]_2$ proceeded rapidly at 25°C to form propene, with small amounts of propane, and $\text{C}_3\text{H}_6\text{Fe}(\text{CO})_4$ in addition to $\text{Fe}_3(\text{CO})_{12}$ and the ferracyclopentadiene. 2. Reaction of the allyliron dimer with butadiene gave $\eta^4\text{-C}_4\text{H}_6\text{Fe}(\text{CO})_3$.

Introduction

Dinuclear metal complexes may be considered as cluster prototypes and may in their chemistry provide insights to reactions that occur on metal surfaces. The extent of the metal-metal interaction in these dimers varies quite extensively. There are the robust dimers with quadruple^{2,3} and triple^{2,4} bonds, two classes that have been extensively investigated in a structural context and which exhibit reactivities that might be exploited in a catalytic context. There is a presently smaller class of dimers that appears to have metal-metal double bonds.⁵ Finally, there is a large class in which there is nominally a single metal-metal bond. In this last class, the metal-metal bond is often the weakest in the dimeric molecule. One contributing factor to the metal-metal bond fragility is the nonbonding repulsion forces generated by the plethora of ligands typically attached to the metal atoms in this class of dimers. Thus, the chemistry of these dimers often may be dominated by a first step dissociative process that generates two mononuclear complexes that usually are 17-electron species. These then would not be models of metal surfaces in chemical reactions. This class does, however, present the possibility of generating reactive mononuclear fragments that could be intermediates in chain reactions. Brown and co-workers⁶ have elegantly demonstrated that 17-electron complexes in some cases display facile ligand dissociation to give very reactive 15-electron species and that such species are often key chain intermediates in radical-initiated substitution reactions of six-coordinate molecules like $\text{HRe}(\text{CO})_5$.

We are exploring the solution chemistry of metal-metal bonded organometallic dimers in an effort to delineate the chemistry of the monomers derived from these dimers. Earlier we established the enthalpy of dissociation of $[\eta^3\text{-C}_3\text{H}_5\text{Fe}(\text{CO})_3]_2$ and several phosphine and phosphite derivatives of this allyliron dimer.⁷ The enthalpies are quite low, 13.5 kcal/mol for the parent tricarbonyl. Hence, the solution chemistry of the monomer $\eta^3\text{-C}_3\text{H}_5\text{Fe}(\text{CO})_3$ is accessible over a wide range of temperatures, -100 to 50°C (above $\sim 50^\circ\text{C}$ rapid thermal decomposition ensues). We describe here the structure for the dimer in the solid state and the solution-phase chemistry of the complex.

Results and Discussion

Description of the Structure. A three-dimensional view of the molecular structure is presented in Figure 1, together with the numbering scheme used to define the interatomic distances and angles listed in Tables I and II, respectively. The molecule is centrosymmetric with a crystallographic inversion center located at the midpoint of the iron-iron bond, implying the antirotational configuration.

The most striking feature of the structure is the very long iron-iron bond distance of $3.138(3) \text{ \AA}$. As the covalent radius of iron is estimated from structural data to be near 1.43 \AA ,⁸ the observed bond distance is nearly 0.3 \AA greater than anticipated. This is the same situation found in bis(tricarbonyl- η^5 -cyclopentadienyl)chromium,⁹ which is structurally very similar to the compound we report. Because of the marked structural

Table I. Interatomic Distances (Å)^{a,b}

Atoms	Distance	Atoms	Distance
Bonded			
Fe(1)-Fe'(1)	3.138 (3)	C(1)-O(1)	1.183 (8)
Fe(1)-C(1)	1.837 (9)	C(2)-O(2)	1.157 (8)
Fe(1)-C(2)	1.778 (9)	C(3)-O(3)	1.149 (7)
Fe(1)-C(3)	1.830 (8)	C(1,1)-C(1,2)	1.417 (5)
Fe(1)-C(1,1)	2.208 (4)	C(1,2)-C(1,3)	1.389 (5)
Fe(1)-C(1,2)	2.104 (4)		
Fe(1)-C(1,3)	2.195 (4)		
Nonbonded			
C(1)-C(2)	2.596 (12)	C(3)-C(1,3)	2.952 (9)
C(1)-C(3)	2.682 (11)	C(3)-C'(1,1)	3.751 (8)
C(1)-C(1,1)	2.853 (9)	C(3)-C'(1,2)	3.276 (8)
C(1)-C(1,3)	2.854 (9)	C(3)-O'(2)	3.476 (10)
C(1)-C(1,2)	3.195 (9)	C(1,1)-C(1,3)	2.435 (6)
C(2)-C(1,1)	2.929 (9)	C(1,1)-O'(3)	3.285 (7)
C(2)-C(3)	2.860 (11)	C(1,2)-O'(2)	3.513 (8)
C(2)-C'(3)	2.990 (11)	C(1,2)-O'(3)	3.474 (7)
C(2)-C'(1,2)	3.288 (9)	C(1,3)-O'(2)	3.374 (8)
C(2)-C'(1,3)	3.431 (9)		
C(2)-O'(3)	3.478 (10)		
C(3)-C'(2)	2.990 (11)		

^a Numbers in parentheses are estimated standard deviations in the last significant digit. ^b Primes indicate inversion related atoms in the opposite half of the molecule.

Table II. Interatomic Angles (deg)^{a,b}

Atoms	Angle	Atoms	Angle
Fe(1)-C(1)-O(1)	176.6 (8)	C(3)-Fe(1)-C(1,1)	160.8 (2)
Fe(1)-C(2)-O(2)	174.3 (8)	C(3)-Fe(1)-C(1,2)	123.5 (2)
Fe(1)-C(3)-O(3)	175.0 (7)	C(3)-Fe(1)-C(1,3)	93.9 (2)
Fe(1)-C(1,2)-C(1,1)	74.8 (2)	C(3)-Fe(1)-Fe'(1)	74.7 (2)
Fe(1)-C(1,2)-C(1,3)	74.7 (2)	C(1,1)-Fe(1)-Fe'(1)	106.8 (1)
C(1)-Fe(1)-C(2)	91.8 (4)	C(1,2)-Fe(1)-Fe'(1)	91.6 (1)
C(1)-Fe(1)-C(3)	94.0 (3)	C(1,3)-Fe(1)-Fe'(1)	107.1 (1)
C(1)-Fe(1)-C(1,1)	89.2 (3)	C(1,1)-C(2)-C(3)	86.9 (3)
C(1)-Fe(1)-C(1,2)	108.2 (3)	C(2)-C(3)-C(1,3)	84.8 (3)
C(1)-Fe(1)-C(1,3)	89.7 (3)	C(3)-C(1,3)-C(1,1)	94.8 (2)
C(1)-Fe(1)-Fe'(1)	160.2 (2)	C(1,3)-C(1,1)-C(2)	93.4 (2)
C(2)-Fe(1)-C(3)	104.8 (3)	C(1,1)-C(1,2)-C(1,3)	120.4 (4)
C(2)-Fe(1)-C(1,1)	93.9 (3)	C(1,1)-Fe-C(1,3)	67.1 (2)
C(2)-Fe(1)-C(1,2)	124.8 (3)		
C(2)-Fe(1)-C(1,3)	161.0 (2)		
C(2)-Fe(1)-Fe'(1)	75.3 (3)		

^a Numbers in parentheses are estimated standard deviations in the last significant digit. ^b Primes indicate inversion related atoms in the opposite half of the molecule.

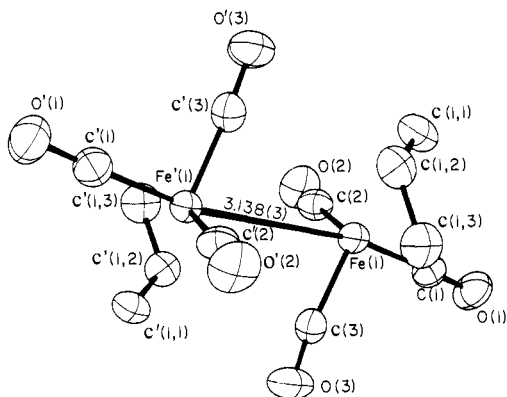


Figure 1. Molecular structure of $[\eta^3\text{-C}_3\text{H}_5\text{Fe}(\text{CO})_3]_2$. Thermal ellipsoids are shown at the 50% probability level.

similarity we believe that the arguments presented to explain the long chromium-chromium distance in that compound are applicable to our material and we refer the reader to ref 9 for

details. Briefly stated, the long metal-metal bond results from the balance between increasing bond strength at short bond distances and the reduced nonbonded repulsions at longer bond distances.

In order to evaluate the role of nonbonded interactions, it is necessary to first discuss the coordination geometry about each iron atom in the dimer. The coordination about each iron atom can be described as pseudooctahedral with the metal-metal bond and one carbonyl ligand (C(1)-O(1)) occupying an axial coordination site and two carbonyl ligands (C(2)-O(2), C(3)-O(3)) and the terminal carbon atoms of the allyl group occupying the equatorial sites. This is justified by a consideration of the angles defined by the ligands surrounding the central iron atom of C(2)-Fe-C(3) = 104.8 (3)°, C(2)-Fe-C(1,1) = 93.9 (3)°, C(3)-Fe-C(1,3) = 93.9 (3)°, C(1,1)-Fe-C(1,3) = 67.1 (2)°, Fe'(1)-Fe(1)-C(1) = 160.2 (2)°. The unusually small (C(1,1)-Fe-C(1,3) = 67.1 (2)°) angle is due to the constricted nature of the allyl group.

The equatorial carbonyl carbon atoms, the terminal carbon atoms of the allyl group, and the iron atom form a plane in which no atoms deviate from the plane by more than 0.039 Å.

A listing of calculated planes through the molecule and deviation from planarity of each atom in the plane is presented in Table III along with distances of important atoms to the planes. It can be seen that the iron atom is displaced very slightly from the plane defined by C(1,1), C(1,3), C(2), and C(3) away from the symmetry-related iron atom. The central carbon atom of the allyl group lies 0.690 Å out of the equatorial plane of the molecule toward the molecular center. A dihedral angle of 47.2° was calculated for the intersection of the plane containing the Fe(1), Fe'(1), C(2), C'(2) atoms and the allylic plane. The allylic plane also describes a dihedral angle of 101.5° with the plane of atoms containing Fe(1), C(2), C(3), C(1,1), C(1,3). The iron-allyl carbon bond distances of 2.208 (4) and 2.195 (4) Å to the terminal carbons and 2.104 (4) Å to the central carbon atoms are comparable to previously published η^3 -allyl metal structures; see Table IV. The iron-carbonyl carbon bond distances of 1.778 (9)–1.837 (9) Å are slightly longer than the values of 1.74–1.77 Å observed in butadieneiron tricarbonyl.¹⁰ The carbon-oxygen bond distances in the carbonyl ligands vary by 0.034 Å but were judged not statistically different.^{11a} Table V represents iron-carbonyl carbon and carbonyl carbon-oxygen bond distances before and after addition of the third cumulant of probability density to the structure factor equation. As can be seen from the table slight changes in bond lengths result; however, the result was again judged to be not statistically significant.

One of the striking features of the geometry of the molecule is the Fe'(1)–Fe(1)–C(1) angle of 160.2 (2)°. This deviation from linearity may be due to short nonbonded interactions within the molecule: both C(1)–C(1,1) and C(1)–C(1,3) = 2.85 Å, and C(2)–C'(3) and C(3)–C'(2) = 2.99 Å. The iron-iron bond is probably the weakest in the coordination sphere about each iron atom and therefore is likely to be the most sensitive to additional steric and electronic factors. Thus, the elongation of the metal-metal bond and the canting of opposing halves of the molecule from each other while retaining a relatively undistorted $\eta^3\text{-C}_3\text{H}_5\text{Fe}(\text{CO})_3$ square pyramidal configuration could be rationalized in terms of facile deformation about the iron-iron bond.

The allyl ligand in a trihapto coordination configuration may be considered to occupy one, two, or three coordination sites of a coordination polygon or polyhedron. Since a tridentate characterization appears generally inappropriate for known η^3 -allylmetal complexes of low or intermediate coordination number, the choice reduces to a unidentate or bidentate representation. A characterization of the ligand as bidentate is somewhat absurd in a purely geometric construct because there are *three* ligating carbon atoms in an η^3 -allyl ligand; however, in a molecular orbital view, a bidentate representation is rational especially if the other ligand-metal-ligand angles are close to 90° as in a nominally square planar or octahedral complex—in these instances orthogonal metal orbitals can substantially interact with the π orbitals of the allyl ion. Thus, all $d^8\text{-}\eta^3\text{-C}_3\text{H}_5\text{ML}_2$ complexes have near 90° L–M–L angles unless the ligands are large and generate significant ligand-ligand nonbonding interactions, and clearly these d^8 complexes are best represented as square planar *pseudo*-four-coordinate complexes with bidentate allyl ligands (see Table IV). In $\eta^3\text{-C}_3\text{H}_5\text{Ir}[\text{P}(i\text{-C}_3\text{H}_7)_3]_2$ the P–Ir–P angle is large, 110°, presumably due to minimization of phosphine ligand-phosphine ligand nonbonded interactions. There is only one crystallographically defined $\eta^3\text{-C}_3\text{H}_5\text{ML}_3$ species, a d^8 -allylnickel complex which seems to be reasonably well described as square pyramidal, *pseudo*-five-coordinate with a bidentate allyl ligand. This class of d^8 -square pyramidal allyl complexes should prove relatively common and include, for example, the $\eta^3\text{-C}_3\text{H}_5\text{CoL}_3$ species. All $d^6\text{-}\eta^3\text{-C}_3\text{H}_5\text{ML}_4$ complexes have near 90° L–M–L angles and are best represented as octahedral, *pseudo*-six-coordinate complexes (Table IV) as in the

Table III. Calculated Best Planes through Molecule and Distances of Selected Atoms to Planes

Plane	Atoms in plane	Deviation from plane, Å
1	Fe(1)	0.000
	Fe'(1)	0.000
	C(2)	0.000
	C'(2)	0.000
2	C(1,1)	0.000
	C(1,2)	0.000
	C(1,3)	0.000
3	Fe(1)	0.039
	C(2)	–0.002
	C(3)	–0.023
	C(1,1)	–0.020
4	C(1,3)	0.005
	C(2)	0.011
	C(3)	–0.011
	C(1,1)	–0.013
	C(1,3)	0.013

Atom	Plane	Distance to plane, Å
C(1,1)	1	–2.114
C(1,2)	1	–1.710
C(1,3)	1	–0.700
Fe(1)	2	1.788
C(2)	2	2.860
Fe'(1)	3	–2.872
C(1,2)	3	–0.690
C(1,3)	3	–0.020
C(1,3)	3	0.005

$[\eta^3\text{-C}_3\text{H}_5\text{Fe}(\text{CO})_3]_2$ structure described above. The d^6 bisallylruthenium complex, $(\eta^3\text{-C}_3\text{H}_5)_2\text{Ru}[\text{P}(\text{C}_6\text{H}_5)_3]_2$, has a near-tetrahedral P–Ru–P angle presumably for the same reason that the above-described allyliridium bisphosphine complex has a similar P–Ir–P angle. Notably, an analogous d^6 bisallyl complex, $[(\eta^3\text{-C}_3\text{H}_5)_2\text{RhCl}_2]_2$, with the smaller chloride ligands has been described as an octahedral complex, although angles and atomic positions have not been reported. In the remaining higher coordinate allylmetal complexes, the allyl ligand would seem to be better represented as a unidentate ligand; e.g., in $d^4\text{-C}_3\text{H}_5\text{ML}_5$ complexes the L–M–L angles are near 90° and the coordination polyhedron seems best represented as an octahedron with the allyl ligand *formally* occupying a single coordination site.

In the three idealized electronic and geometric classes of d^8 -square planar, d^6 -octahedral, and d^4 -octahedral with the allyl ligand *formally* portrayed as occupying two, two, and one coordination sites, respectively, there is a general ordering^{11b} of M–C₃H₅ bond lengths of $d^8 < d^6 < d^4$. The d^8 square pyramidal class will probably overlap the d^8 -square planar and d^6 -octahedral classes. Kaduk, Poulos, and Ibers^{11b} recently have neatly summarized these bond distances and bonding features for a variety of η^3 -allylmetal complexes. They define a distance D as the separation between the metal atom and the center of mass of the allyl ligand and a normalized D' value which is equal to D for second- and third-row metals and equal to $D + 0.10$ Å for a first-row metal. These normalized D' distances^{11b} form nonoverlapping ranges for the d^8 -square planar, d^6 -octahedral, and d^4 -octahedral sets of allylmetal complexes. For octahedral d^6 complexes, the range for D' is 1.94–1.99 Å. The D' value for our (allyl)Fe(CO)₃ dimer ($d^7\text{-}d^7$ or d^6) is slightly larger, 2.00 Å, but this value is still outside, although barely, the range (2.02–2.10 Å) reported for d^4 complexes. For the d^8 complexes, the range of normalized distances, D' , is 1.79–1.91 Å.

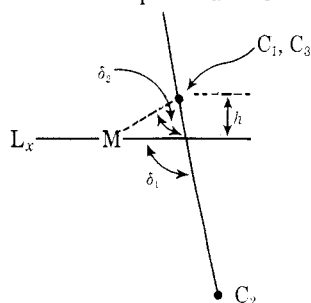
In those instances where a coordination plane for the allylmetal complex can be defined, as by the ML₂ plane in the

Table IV. Structural Data for η^3 -Allyl Complexes

Complex	C.N. ^a	P.F. ^b	MC ₁ ^c	MC ₃ ^c
$[\eta^3\text{-CH}_2\text{C}(\text{CO}_2\text{C}_2\text{H}_5)\text{CH}_2\text{NiBr}]_2$	4	S.P.	2.05 (2)	2.06 (3)
$[\eta^3\text{-C}_3\text{H}_5\text{PdCl}]_2$ (−140 °C)	4	S.P.	2.12 (1)	2.12 (1)
$[\eta^3\text{-CH}(\text{CH}_3)\text{CHCH}(\text{CH}_3)\text{PdCl}]_2$	4	S.P.	2.14 (2)	2.04 (3)
$[\eta^3\text{-CH}_2\text{C}(\text{CH}_3)\text{CH}_2\text{PdCl}]_2$	4	S.P.	2.08 (2)	2.06 (2)
$\eta^3\text{-C}_3\text{H}_5\text{PdC}_{12}\text{H}_{13}\text{NO}^f$	4	S.P.	2.16 (2)	2.11 (2)
$[\eta^3\text{-CH}_2\text{C}(\text{C}_3\text{H}_4\text{Cl})\text{CH}_2\text{PdCl}]_2$	4	S.P.	2.21 (5)	2.19 (5)
$(\eta^3\text{-C}_3\text{H}_5\text{PdCl})_2\text{C}_6\text{H}_{10}\text{NOH}^m$	4	S.P.	2.18 (2)	2.12 (2)
$\{[\eta^3\text{-C}_3\text{H}_5\text{Ni}[\text{SC}(\text{NH}_2)_2]_2]\text{Cl}$	4	S.P.	2.04 (2)	2.07 (2)
$[\eta^3\text{-CH}_2\text{C}(\text{CH}_3)\text{CH}_2]_2\text{Ni}$	4	S.P.		
$\eta^3\text{-C}_3\text{H}_5\text{Pd}[\text{P}(\text{C}_6\text{H}_5)_3](\text{SnCl}_3)$	4	S.P.	2.19 (1)	2.20 (2)
$\eta^3\text{-CH}_2\text{C}(\text{CH}_3)\text{CH}_2\text{Pd}[\text{P}(\text{C}_6\text{H}_5)_3]\text{Cl}$	4	S.P.	2.14	2.28 (3)
$[\eta^3\text{-C}_3\text{H}_5\text{PdOCOCH}_3]_2$	4	S.P.	2.08	2.08
$(\eta^3\text{-C}_3\text{H}_5)_2\text{Ru}[\text{P}(\text{C}_6\text{H}_5)_3]_2$	4,6	T,O	2.25 (2)	2.23 (1)
$\eta^3\text{-CH}_2\text{C}(\text{CH}_3)\text{CH}_2\text{Ni}[(\text{C}_6\text{H}_5)_2\text{PCH}_2]_2\text{Br}$	5	S.Py.	2.06 (1)	2.05 (1)
$\eta^3\text{-C}_3\text{H}_5\text{Pd-}\eta^5\text{-C}_5\text{H}_5$	"5"		2.07	2.10
$\eta^5\text{-C}_5\text{H}_5\text{Ni-}\eta^3\text{-C}_3\text{H}_4\text{-C}_3\text{H}_4\text{-}\eta^3\text{-Ni-}\eta^5\text{-C}_5\text{H}_5$	"5"		1.97 (1)	1.98 (1)
$(\eta^3\text{-C}_3\text{H}_5\text{Ni})_2\text{C}_8\text{H}_6^x$	"5"		2.03 (4)	2.01 (4)
$\eta^3\text{-CH}_2\text{C}(\text{CH}_3)\text{CH}_2\text{Rh}[\text{As}(\text{C}_6\text{H}_5)_3]_2\text{Cl}_2$	6	O	2.25 (2)	2.23 (1)
$\eta^3\text{-C}_3\text{H}_5\text{Fe}(\text{CO})_3\text{I}$	6	O	2.34	2.26
$\eta^3\text{-C}_3\text{H}_5\text{Fe}(\text{CO})_2[\text{P}(\text{C}_6\text{H}_5)_3]\text{I}$	6	O	2.20	2.20
$[(\eta^3\text{-C}_3\text{H}_5)_2\text{RhCl}]_2$	6	O	2.26	2.12
$[(\text{C}_6\text{H}_5)_2\text{B}(\text{pz})_2][\eta^3\text{-CH}_2\text{C}(\text{CH}_3)\text{CH}_2\text{Mo}(\text{CO})_2]$	"6"		2.33 (1)	2.36 (1)
$[(\text{C}_2\text{H}_5)_2\text{B}(\text{pz})_2][\eta^3\text{-CH}_2\text{C}(\text{C}_6\text{H}_5)\text{CH}_2\text{Mo}(\text{CO})_2]$	"6"	O	2.35 (1)	2.31 (1)
$\text{H}_2\text{B}[3,5\text{-(CH}_3)_2\text{pz}]_2[\eta^3\text{-C}_3\text{H}_5\text{Mo}(\text{CO})_2]^{dd}$	7	CO	2.33 (1)	2.36 (1)
$[\eta^3\text{-C}_3\text{H}_5\text{Mo}(\eta^6\text{-C}_6\text{H}_6)\text{Cl}]_2$			2.23 (1)	2.25 (1)
$[\eta^3\text{-C}_3\text{H}_5\text{Mo}]_2[\mu\text{-C}_3\text{H}_5]_2$			2.29 (2)	2.30 (2)
$[\eta^3\text{-C}_3\text{H}_5\text{Cr}]_2[\mu\text{-C}_3\text{H}_5]_2$			2.26	2.24
$[\eta^3\text{-CH}(\text{CH}_3)\text{C}(\text{CH}_3)\text{CH}_2\text{Ti}(\eta^5\text{-C}_5\text{H}_5)_2]$			2.34	2.35
$\eta^3\text{-C}_3\text{H}_5\text{Mo}(\text{NCS})(\text{CO})_2(\text{C}_{10}\text{H}_8\text{N}_2)^{ll}$	6	O	2.29 (1)	2.35 (1)
$\eta^3\text{-C}_3\text{H}_5\text{Mo}(\text{CO})_2(\text{OCOCF}_3)(\text{CH}_3\text{OCH}_2\text{CH}_2\text{OCH}_3)$	6	O	2.34 (2)	2.34 (2)
$\eta^3\text{-C}_3\text{H}_5\text{W}(\text{CO})_2(\text{OCOCF}_3)(\text{CH}_3\text{OCH}_2\text{CH}_2\text{OCH}_3)$	6	O	2.29 (2)	2.29 (2)
$\{\eta^3\text{-C}_3\text{H}_5\text{Ir}(\text{CO})\text{Cl}[\text{P}(\text{C}_6\text{H}_5)_2(\text{C}_6\text{H}_5)]_2\}\{\text{PF}_6\}$	6	O	2.28 (1)	2.25 (1)
$\eta^3\text{-C}_3\text{H}_5\text{Ir}[\text{P}(i\text{-C}_3\text{H}_7)_3]_2$	4	S.P.	2.21 (2)	2.21 (2)

^a C.N., coordination number. With four or fewer additional ligands, the allyl is formally considered a bidentate ligand; with five or more additional ligands, it is considered a monodentate ligand. ^b P.F., polytopal form; S.P., square plane; T, tetrahedron; S.Py., square pyramid; O, octahedron; CO, capped octahedron. ^c M, metal atom; C₂, central allyl carbon atom; C₁ and C₃, terminal allyl carbon atoms. Distances in ångströms. ^d Angle in degrees. ^e δ_1 is the dihedral angle between the plane of the three allyl carbon atoms (C₁C₂C₃) and the plane defined by the metal atom and the two ligand atoms trans to the allyl group (ML₂). δ_2 is the dihedral angle between the C₁C₂C₃ plane and the MC₁C₃ plane. h is the mean distance of the terminal allyl carbon atoms (C₁, C₃) above the ML₂ plane. ^f M. R. Churchill and T. A. O'Brien, *Inorg. Chem.*, **6**, 1386 (1967). ^g A. E. Smith, *Acta Crystallogr.*, **18**, 331 (1965). ^h G. R. Davies, R. H. B. Mais, S. O'Brien, and P. G. Owston, *Chem. Commun.*, 1151 (1967). ⁱ R. Mason and A. G. Wheeler, *J. Chem. Soc. A*, 2549 (1968). ^j C₁₂H₁₃NO, 2-(*R,S*)- α -phenylethylimino-3-penten-4-olato. ^k R. Claverini, P. Ganis, and C. Pedone, *J. Organomet. Chem.*, **50**, 327 (1973). ^l T. A. Broadbent and G. E. Pringle, *J. Inorg. Nucl. Chem.*, **33**, 2009 (1971). ^m C₆H₁₀NOH, cyclohexanone oxime. ⁿ Y. Kitano, K. Kajimoto, M. Kashiwagi, and Y. Kinoshita, *J. Organomet. Chem.*, **33**, 123 (1971). ^o A. Sirigu, *Inorg. Chem.*, **9**, 2245 (1970). ^p H. Dietrich and R. Uttech, *Naturwissenschaften*, **50**, 613 (1963). ^q R. Mason and P. O. Whimp, *J. Chem. Soc. A*, 2709 (1969). ^r R. Mason and D. R. Russel, *Chem. Commun.*, 26 (1966). ^s M. R. Churchill and

d⁸-square planar C₃H₅ML₂ complexes, the general orientation of the allyl ligand in the complex is as shown below, where C₁



and C₃ are the terminal carbon atoms of the allyl ligand. In this definition, the tilt angle, δ_1 , is the angle between the coordination plane and the plane of the allyl ligand (the C₁, C₂, and C₃ carbon atoms). Typically, h , which is an average distance of the C₁ and C₃ carbon atoms from the coordination plane, is a small positive value; the range (Table IV) is from ~ 0 to 0.42 Å. The angle δ_2 is obviously related to δ_1 by h and is always less than δ_1 unless h is zero or negative. Typical values

of δ_1 are in the range of about 105–117° with a value of $\sim 111^\circ$ most commonly found. Two exceptionally large δ_1 values are the 126.5 and 134.1° angles found for two d⁶-octahedral structures (Table IV) with large axial ligands that through L–C₂ nonbonded interactions may be responsible for the larger δ_1 angle. In $[\eta^3\text{-C}_3\text{H}_5\text{Fe}(\text{CO})_3]_2$, the δ_1 angle is unusually small, 98.8°. Most significantly h is negative, -0.13 Å; this displacement may be the result of a minimization of nonbonded intramolecular interactions within the two large allyl Fe(CO)₃ units. With this abnormal displacement of the allyl ligand with respect to the coordination plane, maintenance of a reasonable D' distance (or M–C₁ and M–C₃ distances) requires the δ_1 decrease.

Kaduk, Poulos, and Ibers^{11b} have defined a different tilt angle, τ , as well as a bow angle, β , for the allyl ligand that are independent of the remaining coordination geometry of a complex; their definition would seem a superior one because there is really no ambiguity in their definition—there is no necessity to define a coordination plane. The reader is referred to the Kaduk et al. article for a listing of their τ and β angles. We comment here only on the tilt angle, which is the angle

MC ₂ ^c	C ₁ C ₂ ^c	C ₂ C ₃ ^c	$\angle\text{C}_1\text{C}_2\text{C}_3^d$	$\delta_1^{d,e}$	$\delta_2^{d,e}$	$h^{c,e}$	Ref
1.90 (2)	1.46 (3)	1.45 (3)	119.6 (13)	110.0	100.3	0.27	<i>f</i>
2.11 (1)	1.36 (2)	1.40 (2)	119.8 (9)	111.5 (9)	111.4	0.0	<i>g</i>
2.07 (4)				123,127			<i>h</i>
2.10 (2)	1.37 (3)	1.35 (3)	112.4 (16)	111.6	108.5	0.10	<i>i</i>
2.07 (2)	1.39 (2)	1.41 (3)	116.1 (7)	105.4	103.1	0.08	<i>k</i>
2.12 (5)	1.45 (6)	1.42 (6)	119.0 (38)	117.2	105.1	0.38	<i>l</i>
2.09 (2)	1.32 (4)	1.34 (4)	126.8 (18)	126.5	123.0	0.11	<i>n</i>
				115.8	116.9	-0.03	
1.97 (3)	1.40 (3)	1.33 (3)	123.9 (10)	117.8	108.9	0.26	<i>o</i>
				110(3)			<i>p</i>
2.12 (2)	1.35 (2)	1.38 (3)	129.8 (18)	113.5	113.5	0.0	<i>q</i>
2.22	1.47	1.40		116			<i>r</i>
2.05				117			<i>s</i>
2.13 (1)	1.40 (3)	1.42 (3)	118.2 (13)				<i>t</i>
2.02 (1)	1.42 (2)	1.43 (2)	118.9	106.5			<i>u</i>
2.04	1.35	1.36	117.5				<i>v</i>
1.93 (1)	1.41 (1)	1.41 (1)	111.5 (4)	108			<i>w</i>
1.92 (4)	1.41 (4)	1.41 (4)	118.5 (15)	108.2			<i>y</i>
2.27 (1)	1.44 (2)	1.47 (1)	119.2 (14)	126.6	115.4	0.36	<i>z</i>
2.09	1.35	1.43	131	111.3	99.0	0.40	<i>aa</i>
2.22	1.42	1.40	118	134.1	120.8	0.42	<i>bb</i>
2.17	1.41	1.45		105.5			<i>cc</i>
2.28 (1)	1.43 (1)	1.40 (1)	115 (1)				<i>dd, ee</i>
2.26 (1)	1.41 (1)	1.39 (1)	113.6 (6)				<i>dd, ff</i>
2.21 (1)	1.42 (1)	1.35 (1)	118.4 (4)				<i>gg</i>
2.14 (1)	1.46 (2)	1.45 (2)	112 (1)				<i>hh</i>
2.31 (2)	1.36 (3)	1.40 (2)	120 (2)				<i>ii</i>
2.31	1.46	1.45	121				<i>jj</i>
2.43	1.39	1.38	119.7	124.1			<i>kk</i>
2.20 (1)	1.44 (1)	1.44 (1)	115.7 (11)				<i>mm</i>
2.16 (3)	1.45 (3)	1.45 (3)	144 (3)				<i>nn</i>
2.07 (3)	1.36 (3)	1.36 (3)	123 (3)				<i>nn</i>
2.24 (1)	1.38 (3)	1.40 (3)	125 (2)				<i>oo</i>
2.10 (2)	1.38 (3)	1.32 (3)	129.7 (5)	109.2	109.3	0.0	<i>pp</i>

R. Mason, *Nature (London)*, **204**, 777 (1964). ^t A. E. Smith, *Inorg. Chem.*, **11**, 2306 (1972). ^u M. R. Churchill and T. A. O'Brien, *Chem. Commun.*, 246 (1968). ^v M. Kh. Minasyants and Yu. T. Struchkov, *Zh. Strukt. Khim.*, **9**, 481 (1968). ^w A. E. Smith, *Inorg. Chem.*, **11**, 165 (1972). ^x C₈H₆, dihydropentalenylene. ^y Y. Kitano, M. Kashiwagi, and Y. Kinoshita, *Bull. Chem. Soc. Jpn.*, **46**, 723 (1973). ^z T. G. Hewitt, J. J. DeBoer, and K. Anzenhofer, *Acta Crystallogr., Sect. B*, **26**, 1244 (1970). ^{aa} M. Kh. Minasyants and Yu. T. Struchkov, *Zh. Strukt. Khim.*, **9**, 665 (1968). ^{bb} M. Kh. Minasyants, V. G. Andrianov, and Yu. T. Struchkov, *ibid.*, **9**, 1055 (1968). ^{cc} M. McPartlin and R. Mason, *Chem. Commun.*, 16 (1967). ^{dd} pz, pyrazolyl. ^{ee} F. A. Cotton, B. A. Frenz, and C. A. Murillo, *J. Am. Chem. Soc.*, **97**, 2118 (1975). ^{ff} F. A. Cotton, T. LaCour, and A. G. Stanislawski, *ibid.*, **96**, 754 (1974). ^{gg} C. A. Kosky, P. Ganis, and G. Avitabile, *Acta Crystallogr., Sect. B*, **27**, 1859 (1971). ^{hh} K. Prout and G. V. Rees, *ibid.*, **30**, 2251 (1974). ⁱⁱ F. A. Cotton and J. R. Pipal, *J. Am. Chem. Soc.*, **93**, 5441 (1971). ^{jj} T. Aoki, A. Furusaki, Y. Tomiie, K. Ono, and K. Tanaka, *Bull. Chem. Soc. Jpn.*, **42**, 545 (1969). ^{kk} R. B. Helmholtz, F. Jellinek, H. A. Martin, and A. Vos, *Recl. Trav. Chim. Pays-Bas*, **86**, 1263 (1967). ^{ll} C₁₀H₈N₂, 2,2'-bipyridine. ^{mm} A. J. Graham and R. H. Fenn, *J. Organomet. Chem.*, **17**, 405 (1969). ⁿⁿ F. Dawans, J. Dewailly, J. Meunier-Piret, and P. Piret, *ibid.*, **76**, 53 (1974). ^{oo} Reference 11b. ^{pp} G. Perego, G. D. Piero, and M. Cesari, *Cryst. Struct. Commun.*, **3**, 721 (1974).

Table V. Comparison of Bond Lengths with and without the Third Cumulant of Probability Density Added to the Structure Factor Equation^a

Bond	Distance without 3rd cumulant	Distance with 3rd cumulant
C(1)-O(1)	1.174 (4)	1.183 (8)
C(2)-O(2)	1.135 (5)	1.157 (8)
C(3)-O(3)	1.153 (4)	1.149 (7)
Fe(1)-C(1)	1.848 (4)	1.837 (9)
Fe(1)-C(2)	1.811 (4)	1.778 (9)
Fe(1)-C(3)	1.818 (4)	1.830 (8)

^a Numbers in parentheses are estimated standard deviations in the last significant digit.

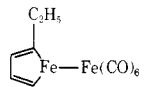
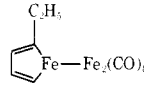
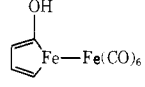
between the vector from the allyl center of mass to C₂ ($\overrightarrow{\text{O}-\text{C}_2}$) and the vector from the center of mass of the ligand to the metal ($\overrightarrow{\text{O}-\text{M}}$). The τ values vary widely, 97–132°, and do not exhibit the relatively narrow range calculated for δ_1 values. The value of τ calculated for $[\eta^3\text{-C}_3\text{H}_5\text{Fe}(\text{CO})_3]_2$ was 112.2°, which is an intermediate value with respect to a range^{11a} found for other allylmetal complexes. Perhaps the δ_1 value despite

the tactical problem in defining a coordination plane is a more informative measure than τ about subtle distortions from "normal" tilt angles.

One point is now clear. It should be possible to rather accurately predict distances, particularly for the D' values, and geometries for allylmetal complexes if the complex neatly fits into one of the categories of $d^8\text{-}\eta^3\text{-C}_3\text{H}_5\text{ML}_2$, $d^6\text{-}\eta^3\text{-C}_3\text{H}_5\text{ML}_4$, or $d^4\text{-}\eta^3\text{-C}_3\text{H}_5\text{ML}_5$. If the L ligands are electronically or sterically diverse, the prediction may be less accurate but trends in tilt and bow angles of the allyls should be anticipated fairly accurately.

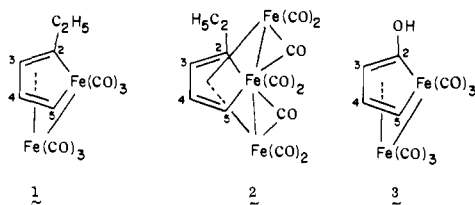
Solution-Phase Decomposition of $[\eta^3\text{-C}_3\text{H}_5\text{Fe}(\text{CO})_3]_2$. Solutions of $[\eta^3\text{-C}_3\text{H}_5\text{Fe}(\text{CO})_3]_2$ in saturated hydrocarbons are unstable. After 24 h, essentially all the allyliron complex was decomposed. Other reactions continue slowly after this point and within 1–2 weeks all reactions appeared complete. The solvent is not involved in the reaction since the use of deuterated solvents did not lead to any products that contained deuterium. Ordinary laboratory light had no effect upon the reaction; sealed reaction vessels maintained in the dark yielded essentially the rate and product characteristics of those for sealed vessels exposed to laboratory light.

The fully characterized products of the solution phase decomposition with appropriate isolated yields (moles) normalized to a hypothetical 10-mol quantity of $\eta^3\text{-C}_3\text{H}_5\text{Fe}(\text{CO})_3$ monomer were as follows.

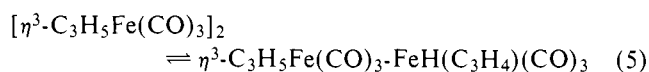
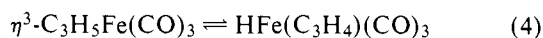
1.6	Fe(metal)	0.07	$\text{Fe}_3(\text{CO})_{12}$	
0.2	CO			
7.3	propylene	0.5		(1)
2.2	$\text{Fe}(\text{CO})_5$	0.7		(2)
		0.6		(3)

In addition, there were small amounts of uncharacterized iron carbonyl clusters (no organic ligands present). No hexadienes were detected in the reaction mixtures. Essentially no differences in product distribution were detected in the solution-phase decomposition effected in sealed tubes and in open (with slow nitrogen purge) vessels.

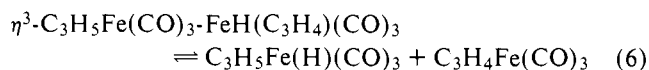
The ferracyclopentadiene complexes, **1–3**, are effectively



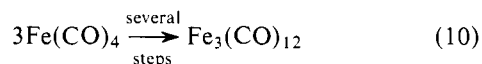
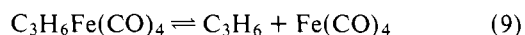
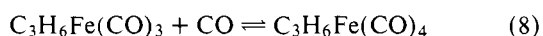
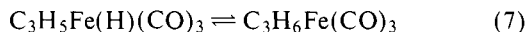
derived from one C_3H_4 or two C_3H_4 species. Hence, hydrogen abstraction must occur at some step. The total number of equivalents of H (abstraction) required to account for these ferracyclopentadienes was ~ 3 which was about one-half the number of equivalents of propylene that was isolated. Hydrogen abstraction may occur in a reversible fashion in the monomeric allyliron complex as shown in eq 4 or in the dimer, eq 5.



Hydride hydrogen transfer between iron atoms could then yield the key mononuclear fragments:

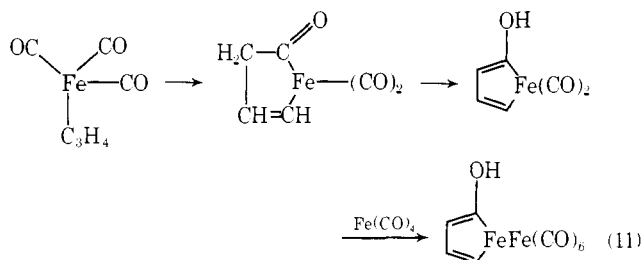


Propylene and iron carbonyls could then be produced through steps 7–10.

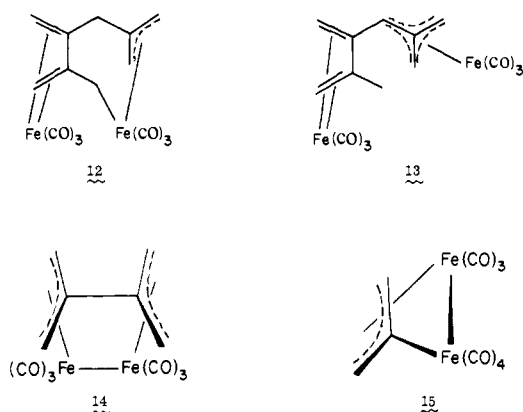


In fact, the propylene complex, $\text{C}_3\text{H}_6\text{Fe}(\text{CO})_4$, was isolated, and characterized, from the solution-phase decomposition products when the reaction was analyzed after 24 h, and it was demonstrated that solutions of the propylene complex yield propylene and $\text{Fe}_3(\text{CO})_{12}$ on standing (absence of CO) in solution at 20 °C.

The $\text{C}_3\text{H}_4\text{Fe}(\text{CO})_3$ species could intramolecularly generate ferracyclopentadiene complex **3** by reaction 11 and could



generate the two other ferracyclopentadienes by multistep interactions with the $\text{C}_3\text{H}_5\text{Fe}(\text{CO})_3$ monomer or dimer. The C_3H_4 moiety bonded to the iron atom in such intermediates could be allene, methylacetylene, or a carbene, $-\text{CH}=\text{CH}=\text{CH}_2$; the latter can be generated in one step from an allyliron complex. Allene itself has been shown to react with $\text{Fe}_3(\text{CO})_{12}$ to give C_9H_{12} and C_6H_8 derivatives¹² of iron as illustrated in **12**, **13**, and **14** and also allene reacts¹³ with $\text{Fe}_2(\text{CO})_9$ to give C_6H_8 and C_3H_4 derivatives² illustrated in



structures **14** and **15**.

None of the ferracyclopentadiene complexes **1**, **2**, and **3** was detected in the reactions of allene with $\text{Fe}_3(\text{CO})_{12}$ and $\text{Fe}_2(\text{CO})_9$. We repeated the allene- $\text{Fe}_2(\text{CO})_9$ reaction and could find no trace of complexes **1–3**. Also we find no evidence for the formation of complexes **12–15** in the solution-phase decomposition of $[\eta^3\text{-C}_3\text{H}_5\text{Fe}(\text{CO})_3]_2$.

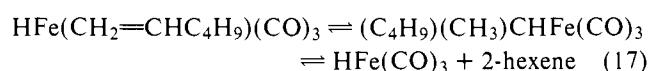
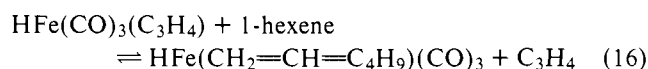
The characterization of the ferracyclopentadienes **1–3** rests on NMR, IR, and mass spectral analyses as well as independent synthesis and the preparation of derivatives. Proposed structures are illustrated above. Structure **1** has been established for the ferracyclopentadiene and methylferracyclopentadiene ring systems by x-ray analysis.¹⁴ We also synthesized **1** by a reaction analogous to a known synthesis procedure for such heterocyclic iron ring structures, namely, the reaction $\text{Fe}_3(\text{CO})_{12}$ and 2-ethylthiophene.¹⁴ Compound **2** is simply a trinuclear analogue of **1** and the structure has been established for the tetraphenylferracyclopentadiene analogue by x-ray analysis.¹⁵ Compound **3** is simply an analogue of **1** with a 2-hydroxy rather than 2-ethyl substituent. Methylation of **3** gave the *O*-methyl derivative, $\text{CH}_3\text{OC}_4\text{H}_3\text{Fe}(\text{CO})_3\text{Fe}(\text{CO})_3$.

Hydrogenation of the Allyliron Complex. Reaction of the allyliron complex with hydrogen is complete within less than 1 h at 20 °C. The primary product was (propylene) $\text{Fe}(\text{CO})_4$, which is unstable and slowly produces propylene, $\text{Fe}_3(\text{CO})_{12}$, and iron metal. Propane (19:1 propylene-propane) and small amounts of the above described solution-phase decomposition products of the allyliron complex were also detected. It was not possible to distinguish between hydrogen reaction with the allyliron monomer or dimer. Either reaction mode should yield $\text{HFe}(\text{C}_3\text{H}_5)(\text{CO})_3$, which could then yield the observed products by the previously cited sequences 7–10. Also possible is the oxidative addition of hydrogen to $\text{C}_3\text{H}_6\text{Fe}(\text{CO})_3$ to give

$\text{C}_3\text{H}_6\text{FeH}_2(\text{CO})_3$ which then could yield propane, an observed minor product.

Catalytic and Exchange Reactions of the Allyliron Complex. Solutions of $[\eta^3\text{-C}_3\text{H}_5\text{Fe}(\text{CO})_3]_2$ rapidly effect isomerization of olefins at 20 °C. 1-Hexene or 2-hexene was converted to a near equilibrium distribution of hexenes within 1 h. This isomerization when effected in deuterated alkane solvents did not lead to hexenes that contained deuterium. Allene was polymerized by such solutions at 20°C; the yields of the air-reactive polymer $(-\text{C}(\text{=CH}_2)\text{CH}_2)_x$ were 50 and 90% after 1 and 14 h, respectively. In contrast, the allyliron complex did not catalyze the polymerization of vinyl monomers.

For the isomerization of hexenes, it is difficult to envisage a plausible catalytic cycle in which the integrity of the allyliron group is maintained throughout the cycle. However, if an $\text{HFe}(\text{CO})_3(\text{C}_3\text{H}_4)$ species were generated (vide supra) by internal hydrogen abstraction then there would be a facile entry to a catalytic cycle:



Alternatively and more likely, the $\text{C}_3\text{H}_6\text{Fe}(\text{CO})_3$ intermediate derived from the solution-phase decomposition product of $[\text{C}_3\text{H}_5\text{Fe}(\text{CO})_3]_2$ could react with a hexene to give (hexene)- $\text{Fe}(\text{CO})_3$ which should rapidly lead to isomerized hexenes through π -allyliron hydride intermediates as demonstrated in the classic study by Casey and Cyr¹⁶ of $\text{Fe}_3(\text{CO})_{12}$ -initiated isomerization of alkenes. Either a $\text{C}_3\text{H}_4\text{Fe}(\text{CO})_3$ or $\text{C}_3\text{H}_6\text{Fe}(\text{CO})_3$ species could be effective in the allene polymerization. This polymerization, however, is rather extensive within minutes at 25 °C, which suggests some initial and relatively fast interaction of $\eta^3\text{-C}_3\text{H}_5\text{Fe}(\text{CO})_3$ and allene.

Reaction of $[\eta^3\text{-C}_3\text{H}_5\text{Fe}(\text{CO})_3]_2$ with butadiene to give $\eta^4\text{-C}_4\text{H}_6\text{Fe}(\text{CO})_3$ was a slow reaction at 20 °C and was competitive to the above described thermal decomposition reaction of the allyliron complex. Thus the dimer is not a clean source of $\text{Fe}(\text{CO})_3$ or an $\text{Fe}(\text{CO})_3$ precursor.

Experimental Section

All operations were conducted with Schlenk techniques under nitrogen or in an inert atmosphere box under argon. Reagent grade solvents were dried by refluxing over appropriate drying agents in a nitrogen atmosphere, lithium aluminum hydride in the case of hydrocarbons and sodium benzophenone ketyl for ethers and aromatic hydrocarbons.

Infrared spectra were recorded with a Perkin-Elmer 337 spectrophotometer. NMR data were obtained with a Varian EM-390 operated at 90 MHz with internal Me_4Si lock. Mass spectra were run by Cornell Mass Spectrometry Facility with an AEI-MS9 (70 eV) or with a Finnegan 330 GC/MS. Analyses of organic compounds were obtained by GLC with a Perkin-Elmer 990 gas chromatograph equipped with a flame ionization detector.

Elemental analyses were obtained from Pascher Mikroanalytisches Laboratorium, Bonn, Germany.

Preparation of $\eta^3\text{-C}_3\text{H}_5\text{Fe}(\text{CO})_3\text{Br}$. A slurry of 10 g (25.5 mmol) of $\text{Fe}_2(\text{CO})_9$ and 7.25 g (60 mmol) of allyl bromide in 200 mL of hexane was stirred for 24 h at room temperature. The reaction mixture was filtered, and the solid residues were washed with two 50-mL portions of hexane. The combined filtrate and washes were evaporated to ca. 100 mL and the concentrate was held at -20 °C for 24 h. Brown crystals formed, and these were collected by filtration and dried under vacuum, 3.0 g (42%).

Preparation of $[\eta^3\text{-C}_3\text{H}_5\text{Fe}(\text{CO})_3]_2$. A reaction slurry of 5.0 g (19 mmol) of $\eta^3\text{-C}_3\text{H}_5\text{Fe}(\text{CO})_3\text{Br}$ and 3 g of zinc dust in 150 mL of ether was stirred vigorously. The solution turned dark red and then yellow-brown over a 2-h period. Excess zinc was then removed by filtration and a second 5.0-g portion of $\eta^3\text{-C}_3\text{H}_5\text{Fe}(\text{CO})_3\text{Br}$ was added. The reaction mixture turned red immediately and was stirred for 0.5

h. The dark red solution was filtered, and the solvent was removed from the filtrate under vacuum to give a dark oily residue. The residue was extracted with two 150-ML portions of pentane; each extraction was vigorously stirred for 15 min before decantation. The combined extracts were filtered. The filtrate was evaporated to 150 mL, and the filtrate was cooled to -78 °C. After ca. 1 h, a crop of dark red crystals was removed by filtration and was dried under vacuum at -78 °C for 12 h, 3.0 g (43%). This reaction proceeded equally well when 0.5% $\text{Na}(\text{Hg})$ was employed as reducing agent, although reaction times were reduced to ca. 10 min. and the reduction did not appear to stop at the anion $[\eta^3\text{-C}_3\text{H}_5\text{Fe}(\text{CO})_3]^-$.

Closed System Solution Decomposition of $[\eta^3\text{-C}_3\text{H}_5\text{Fe}(\text{CO})_3]_2$. A solution of 2.0 g (5.5 mmol) of $[\eta^3\text{-C}_3\text{H}_5\text{Fe}(\text{CO})_3]_2$ in 200 mL of pentane was thoroughly degassed by several freeze-evacuate-thaw cycles and then stirred at room temperature. The initial dark red solution turned greenish-brown after 24 h and solids began to appear. Separation procedures were started after 21 days. The pentane was removed on a vacuum line and collected in a -196 °C trap. Volatiles passing this trap were collected with a Toeppler pump. Carbon monoxide (0.2 mmol) was determined volumetrically. The pentane collected in the -196 °C trap gave a yellow solution when warmed and the presence of $\text{Fe}(\text{CO})_5$ was confirmed by IR. Vacuum distillation of the pentane at -78 °C left 480 mg of $\text{Fe}(\text{CO})_5$. The pentane distillate, trapped at -196 °C, contained 8.0 mmol of propene by GLC analysis (6 ft \times 1/8 in. 15% dimethylsulfolane). No hexadienes were detected by GLC (a series coupled set based on 12 ft \times 1/8 in. 3% squalane and 7 ft \times 1/8 in. 20% ethyl *N,N*-dimethylloxamate).

The solid reaction residues were extracted with five 50-mL portions of pentane which left 300 mg of black solid. The filtered extracts were combined and stripped to ca. 50 mL. A crop of dark green solid, 350 mg, was removed by filtration and the filtrate evaporated to a dark, oily residue.

The oily residue was redissolved in 20 mL of pentane. The solution was divided into four equal portions, and each was chromatographed on a silica gel (activated at 120 °C for 24 h) column, 300 \times 25 mm. Elution with 50% (v/v) benzene in hexane gave four incompletely resolved bands (yellow-green-brown-green) which were collected together, fraction 1. Elution with ether gave a bright yellow band, fraction 2, and a final wash with acetonitrile gave a reddish-brown band, fraction 3. The respective fractions from each portion of the reaction mixture were combined and the solvents were removed by evacuation.

Fraction 1 was redissolved in 5 mL of hexane which was rechromatographed on silica gel, 300 \times 25 mm (slow elution with hexane). Band 1a, yellow, was incompletely resolved from band 1b, green. The combined yellow-green band was split in the center and each half was collected. Band 1c, brown and diffuse, bled slowly off the column while band 1d, dark green, was more slowly eluted. Band 1a was separated from traces of 1b by chromatography on alumina (grade I), 150 \times 10 mm, eluting with 10% (v/v) benzene in hexane. Solvent removal gave ca. 200 mg (10%) of red-orange oil which was further purified by vacuum distillation at 40 °C to a 0 °C probe. This material was tricarbonyl[tricarbonyl-(2-ethylferracyclopentadiene)]iron (**1**): IR (ν_{CO} , hexane) 2075 (m), 2035 (s), 2000 (s), 1995 (s), 1950 cm^{-1} (w); NMR (δ (C_6D_6 , Me_4Si) H_4 , 6.27 (dd, $J_{45} = 5.4$, $J_{43} = 2.4$ Hz (1 H)), H_5 , 5.34 (dd, $J_{54} = 5.4$, $J_{53} = 2.4$ Hz (1 H)), H_3 , 5.11 (t, $J_{34} = J_{35} = 2.4$, $J = 0.6$ Hz (1 H)), $-\text{CH}_2-$, 2.14 (m (2 H)), $-\text{CH}_3$, 0.90 (t, $J = 7.5$ Hz (3 H)); mass spectrum m/e (1) (100 °C sample) 360 (48) $\text{C}_6\text{H}_8\text{Fe}_2(\text{CO})_6$, 332 (26) $\text{C}_6\text{H}_8\text{Fe}_2(\text{CO})_5$, 304 (29) $\text{C}_6\text{H}_8\text{Fe}_2(\text{CO})_4$, 276 (35) $\text{C}_6\text{H}_8\text{Fe}_2(\text{CO})_3$, 248 (100) $\text{C}_6\text{H}_8\text{Fe}_2(\text{CO})_2$, $\text{C}_6\text{H}_8\text{Fe}(\text{CO})_4$, 220 (89) $\text{C}_6\text{H}_8\text{Fe}_2(\text{CO})$, $\text{C}_6\text{H}_8\text{Fe}(\text{CO})_3$, 192 (74) $\text{C}_6\text{H}_8\text{Fe}_2$, $\text{C}_6\text{H}_8\text{Fe}(\text{CO})_2$, 190 (22) $\text{C}_6\text{H}_6\text{Fe}_2$, $\text{C}_6\text{H}_6\text{Fe}(\text{CO})_2$, 169 (14) $\text{C}_2\text{H}_5\text{Fe}(\text{CO})_3$, 164 (12) $\text{C}_6\text{H}_8\text{Fe}(\text{CO})$, 137 (12) C_2HFe_2 , $\text{C}_2\text{HFe}(\text{CO})_2$, 134 (40) $\text{C}_6\text{H}_6\text{Fe}$, 131 (47) $\text{C}_6\text{H}_3\text{Fe}$, 112 (91) Fe_2 , $\text{Fe}(\text{CO})_2$, 81 (12) C_2HFe_2 , 56 (65) Fe.

Band 1b gave a small amount (<10 mg) of a green solid contaminated with **1**, displaying ν_{CO} in the 2050-1950- cm^{-1} region.

Band 1c gave a small amount (<10 mg) of a brown oil, displaying ν_{CO} in the 2050-1950- cm^{-1} region.

Band 1d gave 40 mg of a dark green solid when the solvent was removed and was recrystallized from warm hexane. This material was hexacarbonyl[dicarbonyl(2-ethylferracyclopentadiene)]diiron (**2**): mp 138-139.5 °C; IR (ν_{CO} , hexane) 2055 (m), 2020 (s), 1990 (m), 1975 (m), 1875 (m), 1860 cm^{-1} (m); NMR (δ (C_6D_6 , Me_4Si) H_4 , 7.39 (dd, $J_{45} = 5.4$, $J_{43} = 1.8$ Hz (1 H)), H_3 , 7.18 (t, $J_{34} = J_{35} = 1.8$ Hz (1 H)), H_5 , 2.10 (dd, $J_{54} = 5.4$, $J_{53} = 1.8$ Hz (1 H)), $-\text{CH}_2-$, 1.20 (q,

$J = 6.6$ Hz (2 H)), $-\text{CH}_3$, 0.55 (t, $J = 6.6$ Hz (3 H)); mass spectrum m/e (1) (100 °C sample) 472 (5) $\text{C}_6\text{H}_8\text{Fe}_3(\text{CO})_8$, 444 (32) $\text{C}_6\text{H}_8\text{Fe}_3(\text{CO})_7$, 416 (6) $\text{C}_6\text{H}_8\text{Fe}_3(\text{CO})_6$, 338 (17) $\text{C}_6\text{H}_8\text{Fe}_3(\text{CO})_5$, 360 (67) $\text{C}_6\text{H}_8\text{Fe}_3(\text{CO})_4$, $\text{C}_6\text{H}_8\text{Fe}_2(\text{CO})_6$, 332 (44) $\text{C}_6\text{H}_8\text{Fe}_3(\text{CO})_3$, $\text{C}_6\text{H}_8\text{Fe}_2(\text{CO})_5$, 304 (60) $\text{C}_6\text{H}_8\text{Fe}_3(\text{CO})_2$, $\text{C}_6\text{H}_8\text{Fe}_2(\text{CO})_4$, 276 (47) $\text{C}_6\text{H}_8\text{Fe}_3(\text{CO})$, $\text{C}_6\text{H}_8\text{Fe}_2(\text{CO})_3$, 248 (100) $\text{C}_6\text{H}_8\text{Fe}_3$, $\text{C}_6\text{H}_8\text{Fe}_2(\text{CO})_2$, 220 (87) $\text{C}_6\text{H}_8\text{Fe}_2(\text{CO})$, $\text{C}_6\text{H}_8\text{Fe}(\text{CO})_3$, 192 (71) $\text{C}_6\text{H}_8\text{Fe}_2$, $\text{C}_6\text{H}_8\text{Fe}(\text{CO})_2$, 190 (32) $\text{C}_6\text{H}_6\text{Fe}_2$, $\text{C}_6\text{H}_6\text{Fe}(\text{CO})_2$, 168 (4) Fe_3 , $\text{Fe}_2(\text{CO})_2$, $\text{Fe}(\text{CO})_4$, 164 (9) $\text{C}_6\text{H}_8\text{Fe}(\text{CO})$, 132 (20) C_2HFe_2 , $\text{C}_2\text{HFe}(\text{CO})_2$, 134 (35) $\text{C}_6\text{H}_6\text{Fe}$, 112 (110) Fe_2 , $\text{Fe}(\text{CO})_2$, 81 (14) C_2HFe , 56 (74) Fe. Anal. Calcd for $\text{C}_{14}\text{H}_8\text{Fe}_3\text{O}_8$: C, 35.60; H, 1.71; O, 27.10. Found: C, 34.80; H, 1.84; O, 27.00.

Fraction 2 was redissolved in ether, and the solution was rechromatographed on silica gel (deactivated with ether), 300×25 mm. Elution with ether gave one broad yellow band. Removal of the solvent yielded 200 mg (10%) of a yellow-brown oil which was purified by vacuum distillation at 60 °C to a 0 °C probe. This material was tricarbonyl[tricarbonyl(2-hydroxyferracyclopentadiene)]iron (**3**): IR (ν_{CO} , hexane) 2070 (m), 2035 (s), 2005 (s), 1970 cm^{-1} (m); ν_{OH} (hexane) 3580 (w,b); ν_{OH} (neat) 3575 (m), 3490 (m), 3380 (m,b); NMR δ (C_6D_6 , Me_4Si) H₄, 6.12 (dd, $J_{45} = 5.4$, $J_{43} = 2.7$ Hz (1 H)), OH, 5.33 (s (1 H)), H₅, 4.90 (dd, $J_{54} = 5.4$, $J_{53} = 2.7$ Hz (1 H)), H₃, 4.40 (t, $J_{34} = J_{35} = 2.7$ Hz (1 H)); mass spectrum m/e (1) (35 °C sample) 348 (47) $\text{C}_4\text{H}_4\text{OFe}_2(\text{CO})_6$, 320 (34) $\text{C}_4\text{H}_4\text{OFe}_2(\text{CO})_5$, 292 (29) $\text{C}_4\text{H}_4\text{OFe}_2(\text{CO})_4$, 264 (21) $\text{C}_4\text{H}_4\text{OFe}_2(\text{CO})_3$, 236 (100) $\text{C}_4\text{H}_4\text{OFe}_2(\text{CO})_2$, $\text{C}_4\text{H}_4\text{OFe}(\text{CO})_4$, 208 (76) $\text{C}_4\text{H}_4\text{OFe}_2(\text{CO})$, $\text{C}_4\text{H}_4\text{OFe}(\text{CO})_3$, 180 (74) $\text{C}_4\text{H}_4\text{OFe}_2$, $\text{C}_4\text{H}_4\text{OFe}(\text{CO})_2$, 154 (72) $\text{C}_2\text{H}_2\text{OFe}(\text{CO})_2$, 152 (10) $\text{C}_4\text{H}_4\text{OFe}(\text{CO})$, 151 (14) $\text{C}_4\text{H}_3\text{OFe}(\text{CO})$, 128 (39) Fe_2O , 124 (20) $\text{C}_4\text{H}_4\text{OFe}$, 118 (13) $\text{C}_4\text{H}_4\text{OFe}_2(\text{CO})_6^{2+}$, 112 (36) Fe_2 , $\text{Fe}(\text{CO})_2$, 104 (20) $\text{C}_4\text{H}_4\text{OFe}_2(\text{CO})^{2+}$, 94 (16) $\text{C}_3\text{H}_2\text{Fe}$, 90 (11) $\text{C}_4\text{H}_4\text{OFe}_2^{2+}$, 84 (18) $\text{C}_2\text{H}_4\text{Fe}$, 81 (13) C_2HFe , 56 (73) Fe.

Fraction 3 was redissolved in 50% (v/v) THF in acetonitrile and was rechromatographed on silica gel (THF deactivated), 300×25 mm. Elution with 50% (v/v) THF in acetonitrile gave a red-brown band followed by a red-violet band. In each case solvent removal gave 30–50 mg of oily residues which contained CO (by IR) but no protons (NMR).

The black solid initially removed from the reaction mixture was extracted with 50% (v/v) THF in acetonitrile and filtered. A black, magnetic solid, 100 mg, remained which appeared to be iron metal. The filtrate was chromatographed in the same fashion as fraction 3, above, and gave ca. 100 mg each of the red-brown and red-violet materials. These display broad ν_{CO} in the 1980–1950- cm^{-1} region and neither melted nor sublimed under vacuum below 250 °C. These materials darkened above 150 °C.

The green solids isolated by filtration from the concentrated reaction mixture were redissolved in 50% (v/v) benzene in hexane and chromatographed on silica gel, 300×25 mm. Elution with 10% (v/v) benzene in hexane resulted in two bands. The first was blue-green and yielded 50 mg of $\text{Fe}_3(\text{CO})_{12}$ while the second, dark green, gave 300 mg of **2** (340 mg total, 13%).

A closed system reaction was interrupted after 25 h and then worked up: 0.55 g (1.5 mmol) of the dimer was dissolved in 25 mL of pentane, degassed, and left stirring at room temperature for 24 h. The red color of the dimer was slowly discharged over this period and resulted in a yellow-brown solution and some dark solids. The pentane and volatile reaction products were vacuum distilled at room temperature through -22 (CCl_4 slush) and -196 °C traps. Pentane and a yellow material collected in the -196 °C trap while an orange compound slowly collected in the -22 °C trap. The orange material was condensed into an NMR tube containing 0.25 mL of dried and degassed benzene- d_6 (10% v/v, Me_4Si), the tube sealed, and the NMR spectrum recorded. No proton resonances were observed; the sample decomposed in 24 h and gave a pale yellow-green solution with some brown solid. An infrared spectrum of the solution indicated the presence of $\text{Fe}(\text{CO})_5$ and $\text{Fe}_3(\text{CO})_{12}$.

The yellow pentane solution in the -196 °C trap was warmed to -78 °C and the pentane was removed by vacuum distillation over a period of 24 h. This left a yellow liquid which was distilled into an NMR tube as above. The initial NMR spectrum measured at ambient probe temperature (34 °C) was identical with that of $\text{C}_3\text{H}_6\text{Fe}(\text{CO})_4$, see below. The sample rapidly turned green and deposited green solids at 34 °C which were identified as $\text{Fe}_3(\text{CO})_{12}$ (IR). Filtration of this mixture gave a solution for which ^1H NMR spectra indicated the presence of **4** and free propene. The amount of propene complex isolated was estimated to be 50 mg.

Open System Solution Decomposition of $[\eta^3\text{-C}_3\text{H}_5\text{Fe}(\text{CO})_3]_2$. This reaction was conducted exactly as that in the closed system except that the pentane solution of the dimer was stirred under a slow (1–2 bubbles/min) N_2 purge. After 21 days, the reaction mixture was separated as detailed above; essentially identical results were obtained.

Hydrogenation of $[\eta^3\text{-C}_3\text{H}_5\text{Fe}(\text{CO})_3]_2$. A solution of 1.0 g (2.8 mmol) of $[\eta^3\text{-C}_3\text{H}_5\text{Fe}(\text{CO})_3]_2$ in 50 mL of pentane in a 200-mL bulb was degassed, and H_2 was added to the vessel (cooled to -196 °C) such that the pressure of the system was 1 atm. The flask was sealed, warmed to room temperature, and stirred vigorously for 1 h. The red color of the dimer was completely discharged and left a yellow-brown solution with much dark solid. The pentane was removed by vacuum distillation and collected in a trap cooled to -196 °C. A yellow material codistilled with the pentane and gave a yellow solution when the trap contents were warmed to -78 °C. An IR spectrum of this solution suggested the presence of $\text{C}_3\text{H}_6\text{Fe}(\text{CO})_4$ and GLC indicated free propene and propane (95:5). The pentane was removed from the yellow solution by vacuum distillation at -78 °C over 24 h. The yellow liquid which remained in the trap was examined by IR, NMR, and mass spectrometry. All spectral data were consistent with $\text{C}_3\text{H}_6\text{Fe}(\text{CO})_4$: IR (ν_{CO} , pentane) 2075 (w), 2025 (s), 2005 (s), 1980 cm^{-1} (m); NMR δ (C_7D_8 , Me_4Si , -52 °C) H₁, 2.83 (nonbinomial septet, $J_{\text{av}} = 5.5$ Hz (1 H)), H₃, 2.20 (d, $J_{31} = 6.5$ Hz), H₂, 2.00 (d, $J_{21} = 10.5$ Hz (H₃ + H₂ = 2 H)), $-\text{CH}_3$, 1.35 (d, $J_{\text{CH}_3\text{-H}_1} = 4.5$ Hz (3 H)).

Samples of this material left standing at room temperature for 3–4 h were quantitatively converted to $\text{Fe}_3(\text{CO})_{12}$ and propene. Dilute pentane solutions decomposed slowly over 24 h to give $\text{Fe}_3(\text{CO})_{12}$ and a trace of some other green iron carbonyl which displayed ν_{CO} in the 2000–1900- cm^{-1} region.

The nonvolatile residues were separated by chromatography on silica gel in the same fashion as those in the closed system solution decomposition, above, and yielded 50 mg of $\text{Fe}_3(\text{CO})_{12}$, 20 mg of **2**, 15 mg of red-brown material similar to that (band 1c) obtained from the closed system decomposition, and 100 mg of black insoluble residue. Neither **1** nor **3** was formed (<1 mg).

O-Methylation of **3.** The hydroxyl group of **3** was methylated by the method of Sternberg et al.¹⁷ A 75-mg sample of **3** was dissolved in 5 mL of aqueous 0.1 *m* sodium hydroxide, and then 0.15 mL of dimethyl sulfate added. The solution was stirred for 0.5 h and then extracted with five 20-mL portions of ether. The combined extracts were washed with 250 mL of aqueous 0.1 *m* hydrochloric acid in 50-mL portions and dried over anhydrous potassium carbonate, and then the ether was removed. The yellow oil obtained in this fashion was chromatographed on silica gel (deactivated with ether), 300×25 mm, eluting with 10% (v/v) ether in hexane. A single yellow band was collected and gave 50 mg of a yellow oil on removal of the solvent. Spectral data were consistent with the formulation tricarbonyl[tricarbonyl(2-methoxyferracyclopentadiene)]iron (**5**): IR (ν_{CO} , hexane) 2081 (m), 2038 (s), 2011 (s), 1997 (s), 1950 cm^{-1} (w); NMR δ (C_6D_6 , Me_4Si) H₄, 6.23 (dd, $J_{45} = 5.6$, $J_{43} = 2.8$ Hz (1 H)), H₅, 5.04 (dd, $J_{54} = 5.6$, $J_{53} = 2.8$ Hz (1 H)), H₃, 4.40 (t, $J_{34} = J_{35} = 2.8$ Hz (1 H)), $-\text{OCH}_3$, 2.91 (s (3 H)); mass spectrum m/e (1) (40 °C sample) 362 (48) $\text{C}_5\text{H}_6\text{OFe}_2(\text{CO})_6$, 334 (50) $\text{C}_5\text{H}_6\text{OFe}_2(\text{CO})_5$, 306 (36) $\text{C}_5\text{H}_6\text{OFe}_2(\text{CO})_4$, 278 (30) $\text{C}_5\text{H}_6\text{OFe}_2(\text{CO})_3$, 250 (100) $\text{C}_5\text{H}_6\text{OFe}_2(\text{CO})_2$, $\text{C}_5\text{H}_6\text{OFe}(\text{CO})_4$, 222 (88) $\text{C}_5\text{H}_6\text{OFe}_2(\text{CO})$, $\text{C}_5\text{H}_6\text{OFe}(\text{CO})_3$, 194 (91) $\text{C}_5\text{H}_6\text{OFe}_2$, $\text{C}_5\text{H}_6\text{OFe}(\text{CO})_2$, 168 (36) $\text{C}_3\text{H}_4\text{OFe}(\text{CO})_2$, 166 (5), $\text{C}_5\text{H}_6\text{OFe}(\text{CO})$, 151 (22) $\text{C}_3\text{H}_3\text{OFe}(\text{CO})$, 138 (28) $\text{C}_5\text{H}_6\text{OFe}$, 125 (17) $\text{C}_5\text{H}_6\text{OFe}_2(\text{CO})^{2+}$, 112 (29) Fe_2 , $\text{Fe}(\text{CO})_2$, 56 (26) Fe.

Preparation of **1 by an Alternative Procedure.** A sample of **1** was prepared by the method of Hübener and Weiss.¹⁴ A mixture of 15.5 g of $\text{Fe}_3(\text{CO})_{12}$ and 5 mL of 2-ethylthiophene in 150 mL of heptane was heated to reflux temperature for 16 h. The reaction mixture was allowed to cool to room temperature. A large amount of black solid was removed by filtration. The yellow filtrate was passed through a column of alumina (grade 1), 200×45 mm. A yellow band formed and remained fixed at the head of the column. Elution with 10% (v/v) benzene in hexane gave a small yellow band followed by a second larger yellow band. The first band was presumably a thiaferracyclohexadiene which was not isolated. Removal of the solvent from the second band afforded 500 mg of a red oil which was distilled as **1**. The NMR spectrum of this material was identical with that of **1**.

Reactions Catalyzed by $[\eta^3\text{-C}_3\text{H}_5\text{Fe}(\text{CO})_3]_2$. A solution of $[\eta^3\text{-C}_3\text{H}_5\text{Fe}(\text{CO})_3]_2$ (46 mg, 0.12 mmol) in allene (5 g, 12.5 mmol) in a sealed Carius tube reacted rapidly on warming to 20 °C with color

Table VI. Positional Parameters and Anisotropic Temperature Factors for Nonhydrogen Atoms^a

Atom	x	y	z	β_{11}	β_{22}	β_{33}	β_{12}	β_{13}	β_{23}
Fe(1)	0.061 59 (6)	0.465 45 (5)	0.153 70 (5)	0.009 32 (7)	0.008 52 (6)	0.007 16 (6)	0.000 25 (7)	0.000 10 (4)	-0.000 21 (6)
O(1)	0.0679 (7)	0.3417 (6)	0.4504 (6)	0.0242 (6)	0.0108 (4)	0.0144 (4)	0.0008 (5)	0.0029 (4)	0.0024 (4)
O(2)	-0.2649 (7)	0.5598 (6)	0.2099 (7)	0.0150 (6)	0.0154 (5)	0.0182 (5)	0.0030 (4)	0.0044 (4)	-0.0001 (4)
O(3)	0.0242 (6)	0.1771 (6)	0.0198 (6)	0.0247 (6)	0.0160 (5)	0.0081 (4)	0.0011 (4)	0.0010 (4)	-0.0024 (3)
C(1)	0.0695 (9)	0.3878 (8)	0.3331 (9)	0.0125 (6)	0.0110 (6)	0.0088 (5)	0.0009 (6)	0.0012 (4)	-0.0018 (5)
C(2)	-0.137 (1)	0.5238 (8)	0.1805 (8)	0.0118 (6)	0.0109 (6)	0.0095 (5)	0.0014 (5)	0.0002 (5)	0.0004 (4)
C(3)	0.0393 (8)	0.2910 (9)	0.0655 (8)	0.0112 (6)	0.0090 (5)	0.0108 (5)	0.0005 (4)	0.0000 (5)	0.0005 (4)
C(1,1)	0.1720 (5)	0.6655 (4)	0.2377 (4)	0.0171 (7)	0.0134 (6)	0.0082 (4)	-0.0006 (5)	-0.0024 (5)	-0.0008 (4)
C(1,2)	0.2626 (4)	0.6024 (4)	0.1275 (4)	0.0108 (5)	0.0118 (6)	0.001 16 (5)	0.0000 (4)	-0.0036 (4)	0.0006 (4)
C(1,3)	0.3241 (4)	0.4660 (4)	0.1443 (4)	0.0095 (5)	0.0142 (6)	0.0133 (5)	0.0027 (5)	0.0009 (4)	0.0009 (5)

^a Numbers in parentheses are estimated standard deviations in the last significant digit.

Table VII. Third Cumulant Elements for Carbonyl Atoms^{a,b}

Atom	C_{111}	C_{222}	C_{333}	C_{112}	C_{122}	C_{113}	C_{133}	C_{223}	C_{233}	C_{123}
O1	14 (15)	9 (10)	9 (9)	-1 (8)	-10 (8)	19 (8)	13 (6)	0 (6)	6 (6)	10 (5)
O2	-12 (14)	3 (11)	15 (11)	-6 (8)	10 (7)	1 (8)	16 (7)	-2 (6)	-6 (6)	6 (5)
O3	2 (15)	-4 (10)	-11 (7)	-6 (9)	-10 (7)	10 (7)	-8 (6)	1 (6)	-8 (5)	-2 (5)
C(1)	3 (11)	-41 (13)	-20 (9)	1 (8)	10 (9)	-6 (6)	8 (6)	0 (7)	-6 (7)	-4 (6)
C(2)	60 (15)	8 (9)	-2 (8)	-10 (9)	3 (8)	-19 (8)	9 (6)	-6 (6)	2 (5)	-2 (5)
C(3)	39 (12)	-3 (10)	-10 (11)	-6 (7)	-2 (6)	-2 (7)	3 (7)	0 (6)	-5 (7)	-3 (5)

^a Elements multiplied by 10^5 . ^b Numbers in parentheses are estimated standard deviations.

changes from red to green to pale yellow. A 50 and 90% conversion of allene to $(-\text{C}(\text{=CH}_2)\text{CH}_2)_x$ polymer was realized after 1 and 14 h, respectively. The air-sensitive polymer was purified by separation of the crude polymer from hot toluene by addition of *n*-hexane and was identified by its NMR spectrum.¹⁸

$[\eta^3\text{-C}_3\text{H}_5\text{Fe}(\text{CO})_3]_2$ did not catalyze the polymerization (20 °C, sealed Carius tube reactions with N_2 or argon atmosphere, 1:100 complex:monomer ratio) of acrylonitrile, isoprene, ethyl acetate, methyl acrylate, methyl vinyl ketone, and vinyl acetate. A slow polymerization of methyl vinyl ether and styrene occurred over several days.

Sealed Carius tube reactions (N_2 atmosphere) of 1- or 2-hexenes and $[\eta^3\text{-C}_3\text{H}_5\text{Fe}(\text{CO})_3]_2$ at 25 °C yielded near-equilibrium mixtures of hexenes in 1 h determined by GLC on series coupled set of squalane (3%, 12 ft) and ethyl *N,N*-dimethyl oxamate (20%, 7 ft) columns.

Reaction of Butadiene with $[\eta^3\text{-C}_3\text{H}_5\text{Fe}(\text{CO})_3]_2$. A solution of $[\eta^3\text{-C}_3\text{H}_5\text{Fe}(\text{CO})_3]_2$ (500 mg, 1.25 mmol) and excess 1,3-butadiene (saturated solution) in 50 mL of pentane turned from red to light yellow. After 1.5 days, the solvent was removed and a residue was isolated. The residue contained in addition to the typical thermal decomposition products of the dimer a small amount of $\eta^4\text{-C}_4\text{H}_6\text{Fe}(\text{CO})_3$ and a relatively large amount (150 mg) of a brown, nonmagnetic solid that was insoluble in all organic solvents.

Collection and Reduction of X-Ray Data. A multifaceted, approximately spherical crystal which was 0.45 ± 0.03 mm in diameter was selected and sealed under an atmosphere of argon in a soft glass capillary. Preliminary precession photographs showed the crystal to possess Laue symmetry $2/m$ with systematic absences $h0l$, $h + l = 2n + 1$, and $0k0 = 2n + 1$ consistent with the monoclinic space group $P_{21/n}$. The crystal was then transferred to a computer-controlled Picker FACS-I four-circle diffractometer for further analysis. The crystal was of good quality with an ω -scan width at half-height of $0.15\text{--}0.20^\circ$ for several intense reflections.

Thirty reflections above 30° in 2θ were carefully centered and their angle settings refined by a least-squares procedure to obtain accurate cell dimensions at 23 °C. These are $a = 8.356$ (7) Å, $b = 9.400$ (9) Å, $c = 9.315$ (9) Å, $\beta = 91.13$ (2)°, $V = 731.42$ Å³. The calculated density for two molecules per unit cell is 1.643 g/cm³.

Data were collected using Mo $K\alpha$ radiation (0.710 69 Å) from a pyrolytic graphite monochromator (002), a 1.7° take-off angle, and a scintillation counter. A θ - 2θ scan technique with a scan rate of 2° per minute (in 2θ) was used to measure all reflections with $4^\circ \leq 2\theta \leq 55^\circ$. Reflections were scanned from 0.7° below $K\alpha_1$ to 0.7° above $K\alpha_2$. Background counts were measured for 10 s at each end of the scanned range. Three standard reflections were measured every 100 reflections to assess crystal decomposition or movement. No statistically significant drop in the standards was observed.

Two full forms of data were collected. The first data set contained 2764 reflections of which 1443 were judged observed by the criteria $(|F_o|^2) \geq 3\sigma(|F_o|^2)$. This full data set was used in the Patterson and Fourier syntheses and the observed reflections were used in the initial least-squares refinement. Final refinement was based on a "best" data set obtained by averaging equivalent reflections from both forms of data. This procedure reduces the 4583 measured reflections to a set of 2015 unique reflections of which 1675 were "observed" by the criteria of F_o being greater than 1σ . The data were corrected for Lorentz and polarization effects. Absorption corrections were not applied as the multifaceted morphology of the crystal approached sphericity. The maximum discrepancy due to this neglect is estimated to be less than 4%.

Solution and Refinement of the Structure. The structure was refined using full-matrix least-squares techniques minimizing the function $w(|F_o| - |F_c|)^2$, where $|F_o|$ and $|F_c|$ are the observed and calculated structure factor amplitudes, and the weight, w , is $4F_o^2/\sigma^2(F_o^2)$. The agreement indexes R and R_w are defined as $R = \Sigma||F_o| - |F_c||/\Sigma|F_o|$ and $R_w = (\Sigma w(|F_o| - |F_c|)^2/\Sigma w F_o^2)^{1/2}$. The atomic scattering factors for all atoms were obtained from the compilations of Cromer and Waber¹⁹ and the anomalous dispersion terms for iron and oxygen were taken from the compilation of Cromer and Liberman.²⁰

The iron atom was located from a three-dimensional Patterson map.²¹ One cycle of least-squares refinement based on the iron position and using the full data set from the first form of collected data and a unit weighting scheme gave the agreement index $R = 0.450$. The subsequent synthesis of a three-dimensional Fourier map revealed the locations of the remaining nonhydrogen atoms. With the positions of all nonhydrogen atoms input and using a statistical weighting scheme, several cycles of least-squares refinement based on the observed reflections led to the agreement indexes $R = 0.105$ and $R_w = 0.118$.

The synthesis of a difference Fourier map at this point did not unambiguously reveal the location of the allylic hydrogen atoms. Consequently the positions of the hydrogen atoms were input at idealized positions with a C-H bond distance of 0.95 Å. The inclusion of the hydrogen atoms gave after one cycle $R = 0.100$ and $R_w = 0.109$.

Anisotropic thermal parameters were then included and refinement was based on the full averaged data set. During subsequent refinement five low-angle reflections were observed to suffer from extinction problems and were eliminated. Convergence was reached after four cycles of least-squares refinement with agreement indexes $R_w = 0.050$ for all data and $R = 0.052$ and $R_w = 0.048$ for observed data. The "goodness of fit" was 1.33. Subsequently the third cumulant of the probability density function of the structure factor equation was added to the refinement to accommodate any libration or anharmonic motion of the carbonyls that might cause skewness of the carbonyl atoms.²²

Four cycles of least-squares refinement yielded convergence with final agreement indexes $R_w = 0.049$ for all data and $R = 0.069$ and $R_w = 0.049$ for observed data. The final "goodness of fit" was 1.32.

A final difference Fourier contained three peaks of intensity between 0.51 and 0.73 e/Å³ which were associated with the iron atom. No other peaks of intensity greater than 0.50 e/Å³ were observed. The final atomic positional parameters and anisotropic temperature factors are listed in Table VI. Cumulant expansion coefficients for the carbonyl atoms are listed in Table VII. Lists of observed and final calculated structure factor amplitudes and the root mean square amplitudes of thermal vibration are available.²³

Acknowledgment. This research has been supported by the National Science Foundation under Grants NSF DMR-76-01058, MPS-74-2300, and MPS-76-11833 and is gratefully acknowledged by J.J.W., C.F.P., G.D.S., and E.L.M.

Supplementary Material Available: A listing of root-mean-square amplitudes of vibrations and structure factor tables (14 pages). Ordering information is given on any current masthead page.

References and Notes

- (1) (a) Part 12 in this series: E. L. Muetterties, W. R. Pretzer, M. G. Thomas, B. F. Beier, D. L. Thorn, V. W. Day, and A. B. Anderson, *J. Am. Chem. Soc.*, in press. (b) University of Illinois at Urbana-Champaign. (c) Cornell University.
- (2) F. A. Cotton, *Chem. Soc. Rev.*, **4**, 27 (1975).
- (3) F. A. Cotton, B. A. Frenz, J. R. Ebner, and R. A. Walton, *Inorg. Chem.*, **15**, 1630 (1976).
- (4) M. H. Chisholm, F. A. Cotton, M. Extine, M. Millar, and B. R. Stults, *Inorg. Chem.*, **15**, 2244 (1976); *J. Am. Chem. Soc.*, **98**, 4486 (1976); M. H. Chisholm, F. A. Cotton, B. A. Frenz, W. W. Reichert, L. W. Shire, and B. R. Stults, *ibid.*, **98**, 4469 (1976); M. H. Chisholm, F. A. Cotton, M. Extine, and B. R. Stults, *Inorg. Chem.*, **15**, 2252 (1976); **16**, 320, 603 (1977).
- (5) F. A. Cotton, J. D. Jamerson, and B. R. Stults, *J. Am. Chem. Soc.*, **98**, 1774 (1976).
- (6) B. H. Byers and T. L. Brown, *J. Am. Chem. Soc.*, **97**, 947 (1975).
- (7) E. L. Muetterties, B. A. Sosinsky, and K. I. Zamaraev, *J. Am. Chem. Soc.*, **97**, 5299 (1975).
- (8) The covalent radius of iron was estimated in a manner analogous to that used for chromium in ref 9.
- (9) R. D. Adams, D. E. Collins, and F. A. Cotton, *J. Am. Chem. Soc.*, **96**, 749 (1974).
- (10) O. S. Mills and J. Robinson, *Acta Crystallogr.*, **16**, 757 (1963).
- (11) (a) G. H. Stout and L. H. Jensen, "X-Ray Structure Determination, a Practical Guide", Collier-MacMillan, London, 1968, p 419; (b) J. A. Kaduk, A. T. Poulos, and J. A. Ibers, *J. Organomet. Chem.*, **127**, 245 (1977).
- (12) A. Nakamura, P.-J. Kim, and N. Hagihara, *J. Organomet. Chem.*, **3**, 7 (1965); S. Otsuka, A. Nakamura, and K. Tani, *J. Chem. Soc. A*, 154 (1971); N. Yasuda, Y. Kai, N. Yasuoka, and N. Kasai, *J. Chem. Soc., Chem. Commun.*, 157 (1972).
- (13) R. Ben-Shoshan and R. Pettit, *Chem. Commun.*, 247 (1968).
- (14) P. Hübener and E. Weiss, *J. Organomet. Chem.*, **129**, 105 (1977); G. Dettlaf and E. Weiss, *ibid.*, **128**, 213 (1976).
- (15) R. P. Dodge and V. Schomaker, *J. Organomet. Chem.*, **3**, 274 (1965).
- (16) C. Casey and C. Cyr, *J. Am. Chem. Soc.*, **95**, 2248 (1973).
- (17) H. W. Sternberg, R. A. Friedel, R. Markby, and I. Wender, *J. Am. Chem. Soc.*, **78**, 3621 (1956).
- (18) S. Otsuka, K. Mori, T. Sumino, and F. Imaizumi, *Eur. Polym. J.*, **3**, 73 (1967).
- (19) D. T. Cromer and J. T. Waber, "International Tables for X-Ray Crystallography", Vol. IV, Kynoch Press, Birmingham, England, 1974, Table 2.
- (20) D. T. Cromer and D. Liberman, *J. Chem. Phys.*, **53**, 1891 (1970).
- (21) A set of computer programs from Picker Nuclear, Inc., was utilized for automatic operations of the diffractometer. The general plane Fourier mapping program, JIMDAP, modified by J. Ibers and F. Ross from the original version FORDAP by H. Zalkin and D. H. Templeton, was used to calculate Fourier maps. Least-squares programs were a local version of ORFLS by W. R. Busing, K. O. Martin, and H. A. Levy and ORXLS3 based on ORFLS with modifications by R. D. Ellison, W. C. Hamilton, J. A. Ibers, C. K. Johnson and W. E. Thiessen. Standard deviations were calculated using ORFFE3 modified by G. M. Brown, C. K. Johnson and W. E. Thiessen from ORFFE by W. R. Busing, K. O. Martin, and H. A. Levy. ORTEP by C. K. Johnson was used to plot the molecular structures and theoretical hydrogen atom positions were calculated from known atomic positions and hybridizations using HYGEN by F. K. Ross. Angles between planes and deviation from planes were calculated by MEAN PLANE by M. E. Pippy and F. R. Ahmed.
- (22) C. K. Johnson, *Acta Crystallogr., Sect. A*, **25**, 187 (1969).
- (23) Supplementary material.

Photodissociation of Molecular Beams. Cleavage of Metal–Metal Bonds in Rhenium and Manganese Decacarbonyl

Andrew Freedman and Richard Bersohn*

Contribution from the Department of Chemistry, Columbia University, New York, New York 10027. Received December 16, 1977

Abstract: Photodissociation of rhenium decacarbonyl has been studied in a molecular beam. The energy distribution of the photofragments obtained with incident laser light at 300 nm proves that photodissociation involves only metal–metal bond cleavage. Furthermore, two-thirds (~30 kcal/mol) of the available energy is found as internal energy (probably vibrational) of the photofragments, with the balance being translational energy. Angular distributions of the photofragments as a function of polarization of incident light were measured for both rhenium and manganese decacarbonyl. The anisotropy parameter, β , obtained from the distributions has the same value, 1.9 ± 0.3 , in both compounds; this value proves that the first strong ultraviolet absorption bands involve parallel transitions and puts upper limits of several picoseconds on the lifetimes of the excited electronic states.

Photodissociation of a molecular beam offers unique advantages in unraveling the complexities of excited electronic states. These experiments, performed in the gas phase under collision-free conditions, detail the polarization of the involved transition, set limits on the lifetime of the dissociating state, identify the photofragments, and produce information as to energy partitioning in these photofragments without the ambiguities produced by solvent interactions.¹⁻⁶ This technique has been applied to two dimetal decacarbonyls ((CO)₅M–M(CO)₅, M = Re, Mn) whose photochemistry offers unusual synthetic possibilities.⁷⁻¹¹ Both molecules have their first strong

absorption band in the near ultraviolet, the rhenium compound at ~33 000 cm⁻¹ and the manganese compound at ~29 000 cm⁻¹; these transitions are believed to involve excitation and cleavage of the M–M bond.^{10,12}

Experimental Section

The apparatus and experimental procedures have been extensively described elsewhere.^{5,6} In brief, a molecular beam is intersected at right angles by a chopped or pulsed beam of polarized light. A small fraction of molecules are photodissociated; the resulting photofragments are ionized by an electron bombardment ionizer, mass selected